SLAC – PUB – 4121 (Rev.)
April 1987
T/E

Radiative Bhabha Scattering for Singly Tagged and Untagged Configurations*

DEAN KARLEN

Stanford Linear Accelerator Center
Stanford University, Stanford, California, 94305

ABSTRACT

A method for simulating radiative Bhabha scattering for configurations where one or both electrons do not scatter appreciably is presented. Double radiative Bhabha scattering is included by using the equivalent photon approximation. Results from a Monte Carlo event generator are shown for two experimental configurations. When an electron and photon scatter at large angles, the contribution from order α^4 is large for low visible energies. For the single photon configuration, the order α^4 correction is small.

Submitted to *Nuclear Physics B*

* Work supported by the Department of Energy, contract DE – AC03 – 76SF00515.

1. Introduction

Radiative Bhabha scattering where one or both electrons escape detection at low angles is an important background for neutrino counting experiments [1] and some searches for supersymmetry [2] and compositeness [3]. Also, the large cross section allows this process to be used to measure luminosity at e^+e^- machines [4] as well as test QED and radiative corrections.

The Monte Carlo program of Berends and Kleiss [5] simulates Bhabha scattering and includes the order α^3 correction. However, it cannot be used for configurations where an electron scatters at an arbitrarily small angle. So in order to study such configurations, we have produced a program that exclusively simulates radiative Bhabha scattering in this low angle region.

The outline of this paper is as follows. In sect. 2 the process $e^+e^- \to e^+e^-\gamma$ is discussed in lowest order. In sect. 3 the next order radiative correction to this process is treated by using the equivalent photon approximation. In sect. 4 a method to simulate the processes $e^+e^- \to e^+e^-\gamma$ and $e^+e^- \to e^+e^-\gamma\gamma$ by a Monte Carlo procedure is presented. Results from the Monte Carlo program are given in sect. 5.

2. Lowest order process

The lowest order cross section for radiative Bhabha scattering,

$$e^+(p_+)e^-(p_-) \to e^+(q_+)e^-(q_-)\gamma(k) \quad , \tag{2.1}$$

can be expressed in a compact form, in the ultrarelativistic limit, by using the following notation [6,5]:

$$\begin{aligned} &s = (p_+ + p_-)^2\,, \qquad t = (p_+ - q_+)^2\,, \qquad u = (p_+ - q_-)^2\,, \\ &s' = (q_+ + q_-)^2\,, \qquad t' = (p_- - q_-)^2\,, \qquad u' = (p_- - q_+)^2\,, \\ &x_1 = p_+ \cdot k\,, \quad x_2 = p_- \cdot k\,, \quad y_1 = q_+ \cdot k\,, \quad y_2 = q_- \cdot k\,. \end{aligned} \tag{2.2}$$

We are particularly interested in small angle scattering of the electron or positron and hence the quantities, t or t', can be very small. However, terms containing m_e^2/t^2 and m_e^2/t'^2, that could be of the same order as terms containing $1/t$ and $1/t'$, are neglected in the cross section of ref. [5]. To find the m_e^2/t^2 term, we calculated the cross section from the only two diagrams that contribute to such a term, shown in fig. 1. The result was found, using the symbolic manipulation program REDUCE [7], to be

$$d^5\sigma = \frac{\alpha^3}{\pi^2 s}\left(s^2+s'^2+u^2+u'^2+\frac{8m_e^2}{t}(x_2^2+y_2^2)\right)\left(\frac{-1}{x_2y_2t}\right)d^5\Gamma\,,$$
$$d^5\Gamma = \delta^4(p_+ + p_- - q_+ - q_- - k)\,\frac{d^3\mathbf{q}_+}{2q_+^0}\,\frac{d^3\mathbf{q}_-}{2q_-^0}\,\frac{d^3\mathbf{k}}{2k^0}\,, \tag{2.3}$$

in the ultrarelativistic limit. An exact order α^3 calculation [8] of radiative Bhabha scattering was found to contain the same mass term. Including the m_e^2/t'^2 term also, we use for the differential cross section

$$d^5\sigma_{e^+e^-\to e^+e^-\gamma} = d^5\sigma_{\mathrm{BK}} - \frac{\alpha^3}{\pi^2 s}8m_e^2\left(\frac{(x_2^2+y_2^2)}{x_2y_2t^2}+\frac{(x_1^2+y_1^2)}{x_1y_1t'^2}\right)d^5\Gamma, \tag{2.4}$$

where $d^5\sigma_{\mathrm{BK}}$ appears in the appendix. This modification can effect total cross sections by as much as 5% or more when they include electron scattering at arbitrarily small angles.

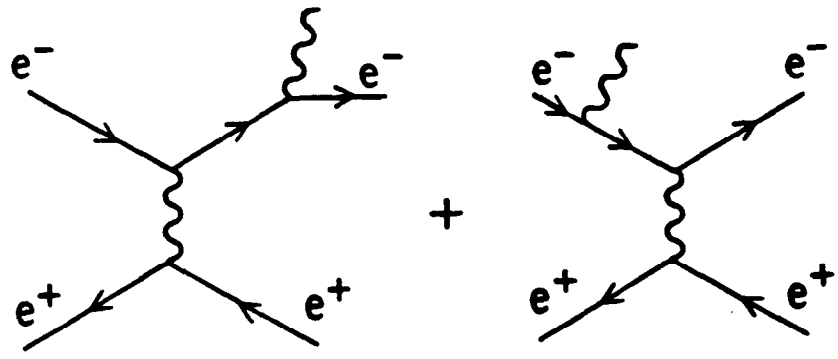

Figure 1. Diagrams that contribute terms containing $1/t$ and m^2/t^2. These and the charge conjugate diagrams dominate the order α^3 cross section for the region under study.

3. Correction to lowest order

In this paper, only the correction from higher order QED will be considered. The contribution from the Z^0 is small since the annihilation channel is significantly reduced by the requirement that an electron be below some small angle in the final state. Matrix elements for double radiative Bhabha scattering are in the literature [9] but a calculation of the virtual correction to radiative Bhabha scattering has not yet been published. So, instead we make use of the equivalent photon approximation [10] (EPA) for the next order correction. With this method, only the diagrams shown in fig. 2 and their charge conjugates are included. This will be shown to be a good approximation of the total radiative correction when one electron scatters at a small angle.

In the following discussion, we consider the diagrams where photons are radiated from the electron while the positron is deflected only slightly. The charge conjugate diagrams are included by symmetrization. Interference between these two sets of diagrams is not included but the net effect is expected to be small. Box diagrams, known to cancel an infrared divergence in the interference terms, are also not included. However, the finite remainder, after the cancellation of the divergence, is small in the similar processes of Møller scattering [11] and two photon pseudoscalar production [12]. In sect. 5 we confirm that the effects of interference and annihilation channel diagrams are small in the lowest order process by simply removing them from the matrix element.

The radiation spectrum from the scattered positron is proportional to [13]

$$\left(\frac{\hat{e}\cdot p_+}{k\cdot p_+}-\frac{\hat{e}\cdot q_+}{k\cdot q_+}\right)^2, \tag{3.1}$$

where k is the momentum of a photon with polarization $\hat{e}$. In the limit that $\mathbf{p}_+$ and $\mathbf{q}_+$ are collinear, the radiation goes to zero and so it is expected that the radiative correction to the positron will be small. This is confirmed by an explicit calculation[14] of the radiative correction to the multiperipheral two

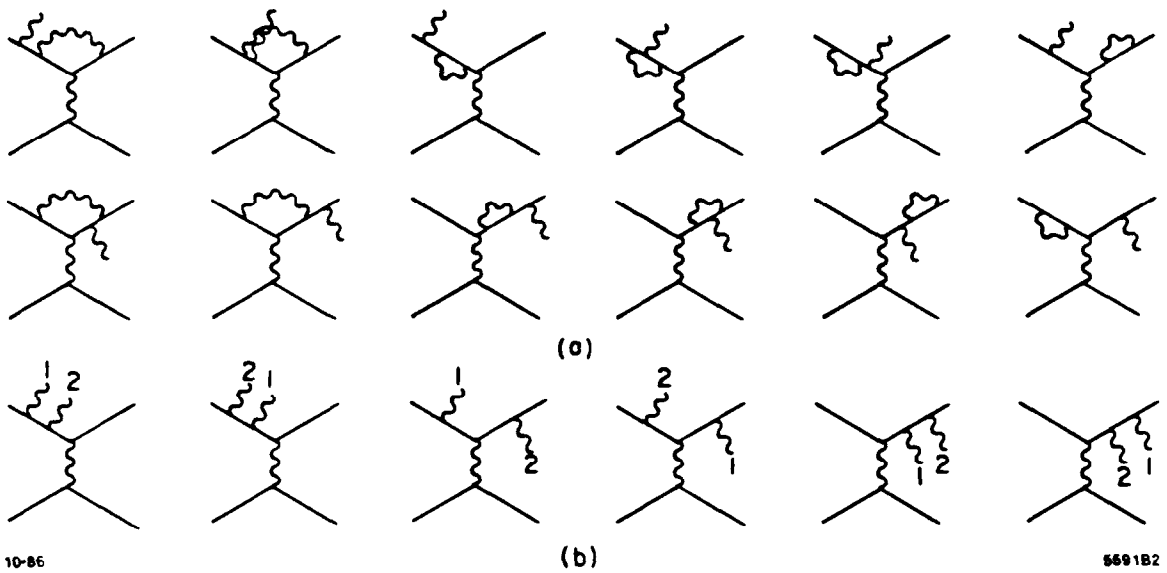

Figure 2. Diagrams included in the approximation of the radiative correction to radiative Bhabha scattering: a) Virtual correction diagrams; b) Double radiative Bhabha diagrams.

photon diagrams of the process, $e^+e^- \to e^+e^-\mu^+\mu^-$. This process is similar to the one studied here, except that both the electron and the positron predominately scatter at small angles. The total correction is found to be on the order of 1%.

Vacuum polarization is also not included since the largest part of the cross section has $q^2 \approx m_e^2$, where the effect is small.

Both virtual and real photon emission from the electron are included in the next order correction. The infrared divergence associated with virtual photon emission is cancelled by integrating the soft real photon emission up to some cutoff energy, $E_{\rm cut}$, leaving a finite correction. This total analytic correction can be written in the form

$$d\sigma^{\rm vs} = (1+\delta)\, d\sigma^{\rm o}, \tag{3.2}$$

where δ depends on the soft photon cutoff energy. The cutoff energy must be small enough that the experimental resolution would not allow the detection of the extra photon and that the approximations used in calculating δ are valid. However, the cutoff energy must be large enough so that $(1+\delta) > 0$ for all of the phase space under study.

The correction term, δ, for radiative Bhabha scattering in the region under study, can be obtained directly from radiative corrections to Compton scattering. The equivalent photon approximation relates these two processes by,

$$d^5\sigma_{e^+e^-\to e^+e^-\gamma} = d^3n_{e^+\to e^+\gamma}\, d^2\sigma_{\gamma e^-\to \gamma e^-} \tag{3.3}$$

where $d^3n_{e^+\to e^+\gamma}$ is the equivalent photon spectrum [10]. The correction, $(1+\delta)$, is thus the same for both processes. This correction term has been calculated for Compton scattering in the γe center of mass system by Mork [15]. Provided that $E_{\rm cut}$ is specified in the γe center of mass system, the corrected cross section is given by

$$d\sigma^{\rm vs}_{e^+e^-\to e^+e^-\gamma} = (1+\delta^{\rm cm}_{\gamma e^-\to \gamma e^-})\, d\sigma_{e^+e^-\to e^+e^-\gamma}, \tag{3.4}$$

where $\delta^{\rm cm}_{\gamma e^-\to \gamma e^-}$ is given in the appendix.

The process, $e^+e^- \to e^+e^-\gamma\gamma$ where both photons have energies greater than $E_{\rm cut}$ in the γe center of mass system, can be calculated by a direct application of the EPA,

$$d^8\sigma_{e^+e^-\to e^+e^-\gamma\gamma} = d^3n_{e^+\to e^+\gamma}\, d^5\sigma_{\gamma e^-\to e^-\gamma\gamma}\,. \tag{3.5}$$

The cross section for double Compton scattering,

$$\gamma(\tilde{k})e^-(p_-) \to e^-(q_-)\gamma(k)\gamma(k_s), \tag{3.6}$$

was first calculated by Mandle and Skyrme [16]. Their result may be written in the form,

$$\begin{aligned} d^5\sigma_{\gamma e^-\to e^-\gamma\gamma} &= \frac{\alpha^3}{\pi^2\tilde{s}}\frac{X_{\rm MS}}{m_e^2}\, d^5\Gamma, \\ d^5\Gamma &= \delta^4(p_- + \tilde{k} - q_- - k - k_s)\,\frac{d^3\mathbf{q}_-}{2q_-^0}\,\frac{d^3\mathbf{k}}{2k^0}\,\frac{d^3\mathbf{k}_s}{2k_s^0}, \\ \tilde{s} &= (p_- + \tilde{k})^2, \end{aligned} \tag{3.7}$$

where $X_{\rm MS}$ is given in the appendix. Then the cross section for double radiative Bhabha scattering,

$$e^+(p_+)e^-(p_-) \to e^+(q_+)e^-(q_-)\gamma(k)\gamma(k_s), \tag{3.8}$$

is given by,

$$\begin{aligned} d^8\sigma_{e^+e^-\to e^+e^-\gamma\gamma} &= \frac{\alpha^4}{\pi^4 s}\frac{X_{\rm MS}}{m_e^2}\left(\frac{-1}{t}\right)\left(\frac{s^2+(s-\tilde{s})^2}{\tilde{s}^2} + \frac{2m_e^2}{t}\right) d^8\Gamma, \\ d^8\Gamma &= \delta^4(p_+ + p_- - q_+ - q_- - k - k_s)\,\frac{d^3\mathbf{q}_+}{2q_+^0}\,\frac{d^3\mathbf{q}_-}{2q_-^0}\,\frac{d^3\mathbf{k}}{2k^0}\,\frac{d^3\mathbf{k}_s}{2k_s^0}, \end{aligned} \tag{3.9}$$

where $\sqrt{\tilde{s}}$ is the γe center of mass energy.

4. Monte Carlo event generation

The Monte Carlo generation follows the method used in ref. [5], where trial events are generated according to an approximate cross section, $d\sigma^{\rm a}$. The trial events are accepted on the basis of the weight,

$$w = d\sigma / d\sigma^{\rm a}, \tag{4.1}$$

so that the final set of events follows the distribution given by $d\sigma$. The total cross section is found by,

$$\sigma = \int w \, d\sigma^{\rm a}. \tag{4.2}$$

For the lowest order process, we use the approximate cross section

$$d^5\sigma^{\rm a}_{e^+e^-\to e^+e^-\gamma} = \frac{\alpha^3}{2\pi^2} \frac{q_+^0}{(1+c+\epsilon)(E_b - q_+^0)^2} \frac{-1}{t} \, d|\mathbf{q}_+| \, d\Omega_{q_+} \, d\Omega_k,$$

$$t = -2E_b q_+^0 \left((1 - \cos\theta_{q_+}) + \epsilon / z_+^{0\,2} \right), \tag{4.3}$$

$$c = \cos\theta_k, \quad \epsilon = \frac{2m_e^2}{s}, \quad z_+^0 = \frac{q_+^0}{E_b - q_+^0},$$

where all angles are measured with respect to $\mathbf{p}_+$. The approximate cross section does not treat electrons and positrons equally. For half of the final events, all charges are reversed, so that the final event sample is charge symmetric.

A good approximation of the double Compton cross section, when $k_s^0 \ll \sqrt{\tilde{s}}$, is [17]

$$d^5\sigma_{\gamma e^-\to e^-\gamma\gamma} \approx \frac{\alpha}{4\pi^2} \left(\frac{p_-}{p_- \cdot k_s} - \frac{q_-}{q_- \cdot k_s} \right)^2 \frac{d^3\mathbf{k}_s}{k_s^0} \, d^2\sigma_{\gamma e^-\to\gamma e^-}. \tag{4.4}$$

By approximating this equation further and again using the EPA, we use the approximate cross section for double radiative Bhabha scattering given by

$$d^8\sigma^{\rm a}_{e^+e^-\to e^+e^-\gamma\gamma} = d^3\sigma^{\rm a}_s \, d^5\sigma^{\rm a}_{e^+e^-\to e^+e^-\gamma},$$

$$d^3\sigma^{\rm a}_s = \frac{\alpha}{4\pi^2}\frac{1}{k_s^{0\,2}}\left(\frac{1}{1-c_{p_-}+\epsilon}+\frac{1}{1-c_{-k}+\epsilon}\right) f(k_s^0,\tilde{s})\,\frac{d^3\mathbf{k}_s}{k_s^0}, \qquad (4.5)$$

$$c_{p_-} = \cos\angle(\mathbf{k}_s,\mathbf{p}_-), \quad c_{-k} = \cos\angle(\mathbf{k}_s,-\mathbf{k}), \quad f(k_s^0,\tilde{s}) = \left(1-\frac{k_s^0}{\frac{1}{2}\sqrt{\tilde{s}}}+\epsilon_s\right)^{-1},$$

where $d^5\sigma^{\rm a}_{e^+e^-\to e^+e^-\gamma}$ is given in eq. (4.3) and $d^3\sigma^{\rm a}_s$ is evaluated in the γe center of mass system. The function, $f(k_s^0,\tilde{s})$, has been included to approximate better the peaking behavior when $k_s^0 \approx \frac{1}{2}\sqrt{\tilde{s}}$ in the γe center of mass system, and ϵ_s is some arbitrary small parameter.

To generate a general phase space variable, x, according to a distribution $D(x)\,dx$, it is necessary to solve the following equation for x:

$$\lambda_i = \int_{x_{\rm min}}^{x} D(\tilde{x})\,d\tilde{x} \Big/ \int_{x_{\rm min}}^{x_{\rm max}} D(\tilde{x})\,d\tilde{x}\,, \qquad (4.6)$$

where λ_i is a random number equidistributed in the interval (0,1). The quantities $x_{\rm min}$ and $x_{\rm max}$ are specified by or calculated from parameters that describe the detector acceptance and event configuration. The photon and electron acceptances are defined by minimum angles with respect to the beam line, $\theta_{\gamma\,\rm min}$ and $\theta_{e\,\rm min}$, and minimum energies, $E_{\gamma\,\rm min}$ and $E_{e\,\rm min}$. Veto angles for photons and electrons are given by the angles, $\theta_{\gamma\,\rm veto}$ and $\theta_{e\,\rm veto}$. All veto angles need not be less than all acceptance angles, however the combination must not allow a collinear final state. The event configurations, identified as $e\gamma$, single γ, and single e, specify the combination of final state particles in the acceptance, the others being below the veto.

From eq. (4.3), the distribution of q_+^0 and $\cos\theta_{q_+}$ is given by

$$D(q_+^0, \cos\theta_{q_+})\, d|\mathbf{q}_+|\, d\cos\theta_{q_+} = \frac{q_+^0}{(E_b - q_+^0)^2}\left(\frac{-1}{t}\right) d|\mathbf{q}_+|\, d\cos\theta_{q_+}. \tag{4.7}$$

The distribution of q_+^0 alone, found by integrating over the positron scattering angle, θ_{q_+}, between 0 and the veto angle, $\theta_{e\,\mathrm{veto}}$, is given by

$$D(z_+^0)dz_+^0 = \frac{2}{s}\frac{q_+^0}{|\mathbf{q}_+|}\ln\left[1 + \frac{(1-\cos\theta_{e\,\mathrm{veto}})}{\epsilon} z_+^{0\,2}\right] dz_+^0. \tag{4.8}$$

Equation (4.6) cannot be solved for this distribution, so z_+^0 is generated by a simple throw away technique. That is, a trial z_+^0 is chosen at random, and is accepted with a probability proportional to $D(z_+^0)$. The second degree of freedom, θ_{q_+}, has the distribution given by eq. (4.7) and is generated by

$$1 - \cos\theta_{q_+} = \frac{\epsilon}{z_+^{0\,2}}\left(\left[1 + \frac{(1-\cos\theta_{e\,\mathrm{veto}})}{\epsilon} z_+^{0\,2}\right]^{\lambda_2} - 1\right). \tag{4.9}$$

Similarly the angle of the photon, θ_k, is generated by

$$1 + \cos\theta_k + \epsilon = (1 + \cos\theta_{\max} + \epsilon)\left(\frac{1 + \cos\theta_{\min} + \epsilon}{1 + \cos\theta_{\max} + \epsilon}\right)^{\lambda_3}, \tag{4.10}$$

where for the $e\gamma$ and single γ configurations, $\theta_{\min} = \theta_{\gamma\,\min}$ and $\theta_{\max} = \pi - \theta_{\gamma\,\min}$, and for the single e configuration, $\theta_{\min} = \pi - \theta_{\gamma\,\mathrm{veto}}$ and $\theta_{\max} = \pi$. The final degrees of freedom for the three body final state are simply

$$\phi_k = 2\pi\lambda_4, \quad \text{and} \quad \phi_{q_+} = 2\pi\lambda_5. \tag{4.11}$$

To generate an event sample which includes the virtual and soft real photon corrections, the factor $(1 + \delta)$ is included in the weight given by eq. (4.1). This sample is combined with the double radiative sample, which is generated separately as shown below, to produce an event sample correct to order α^4.

The double radiative Bhabha event generation closely follows the previous procedure, since the lower order process factors out in eq. (4.5), apart from the term, $f(k_s^0, \tilde{s})$. The distribution of q_+^0 is now given by

$$D(z_+^0)dz_+^0 = \frac{2}{s}\frac{q_+^0}{|\mathbf{q}_+|}\ln\left[1+\frac{(1-\cos\theta_{e\,\mathrm{veto}})}{\epsilon}z_+^{0\,2}\right]\ln r\, dz_+^0,$$
$$r = \frac{\frac{1}{2}\sqrt{\tilde{s}}(1+\epsilon_s) - E_{\mathrm{cut}}}{\epsilon_s E_{\mathrm{cut}}}. \tag{4.12}$$

The remaining degrees of freedom of the three body final state are treated as before leaving just the three degrees of freedom of the second photon. The energy of the second photon in the γe center of mass system is generated by the following algorithm:

$$k_s^{\mathrm{cm}} = \frac{1}{2}\sqrt{\tilde{s}}\,\frac{1+\epsilon_s}{1+\epsilon_s r^{\lambda_6}}. \tag{4.13}$$

The approximate cross section peaks when the second photon is nearly collinear with the initial or final state electron. Since the choice of the axis about which θ_{k_s} and ϕ_{k_s} are measured is arbitrary, by choosing the axis to be along $\mathbf{p}_-$ and $-\mathbf{k}$ alternately, by another random number, both peaks are handled in accordance with eq. (4.5). These angles are generated by

$$1+\cos\theta_{k_s}^{\mathrm{cm}} + \epsilon = \epsilon\left(\frac{2+\epsilon}{\epsilon}\right)^{\lambda_7}, \quad \text{and} \quad \phi_{k_s}^{\mathrm{cm}} = 2\pi\lambda_8. \tag{4.14}$$

5. Results

The methods of the previous section have been incorporated into a Monte Carlo program. In order to make specific comparisons, we have simulated the $e\gamma$ configuration for a typical PEP or PETRA experiment. The invariant mass distribution calculated with this Monte Carlo is shown in fig. 3 compared with a calculation* using the EPA. Removing the annihilation channel and the interference between the t and t' channels changes the total cross section by less than 0.1%. This check was made by using eq. (2.3) instead of eq. (2.4) for the cross section. Hence the approximations used for the next order correction are valid. The choice of the cutoff energy, $E_{\rm cut}$, for the next order correction depends on the detector resolution and analysis criteria. The range of allowed values of $E_{\rm cut}$ is quite wide as shown in fig. 4. Also, the total cross section is shown to not depend on the choice of $E_{\rm cut}$ as required. The total energy inside the acceptance is shown in fig. 5 along with the lowest order result. The total cross section is much larger when the next order diagrams are included due to low visible energy events. In these events, the longitudinal momentum of the missing electron is balanced by a hard photon, also undetected. The total radiative correction can be reduced by requiring that a minimum total energy be detected. Then the order α^4 simulation whould be an accurate representation of this process.

Total cross sections and energy spectra from the lowest order single γ generation agree with results from a numerical integration of the differential cross section† and from another Monte Carlo generator [19] which includes the contribution from the Z^0. In order to judge the effect of including the order α^4

---

* See ref. [4]. We replace eq. (6) by,

$$u_0 = \max\left[\frac{u^\gamma_{\rm min}-\beta}{1-\beta u^\gamma_{\rm min}}, \frac{\beta-u^e_{\rm max}}{1-\beta u^e_{\rm max}}\right] \quad u_1 = \min\left[\frac{u^\gamma_{\rm max}-\beta}{1-\beta u^\gamma_{\rm max}}, \frac{\beta-u^e_{\rm min}}{1-\beta u^e_{\rm min}}\right]$$

† See ref. [18]. The authors chose to use $\alpha = 1/128.5$, whereas we use $\alpha = 1/137.036$. After correcting for this, agreement is found.

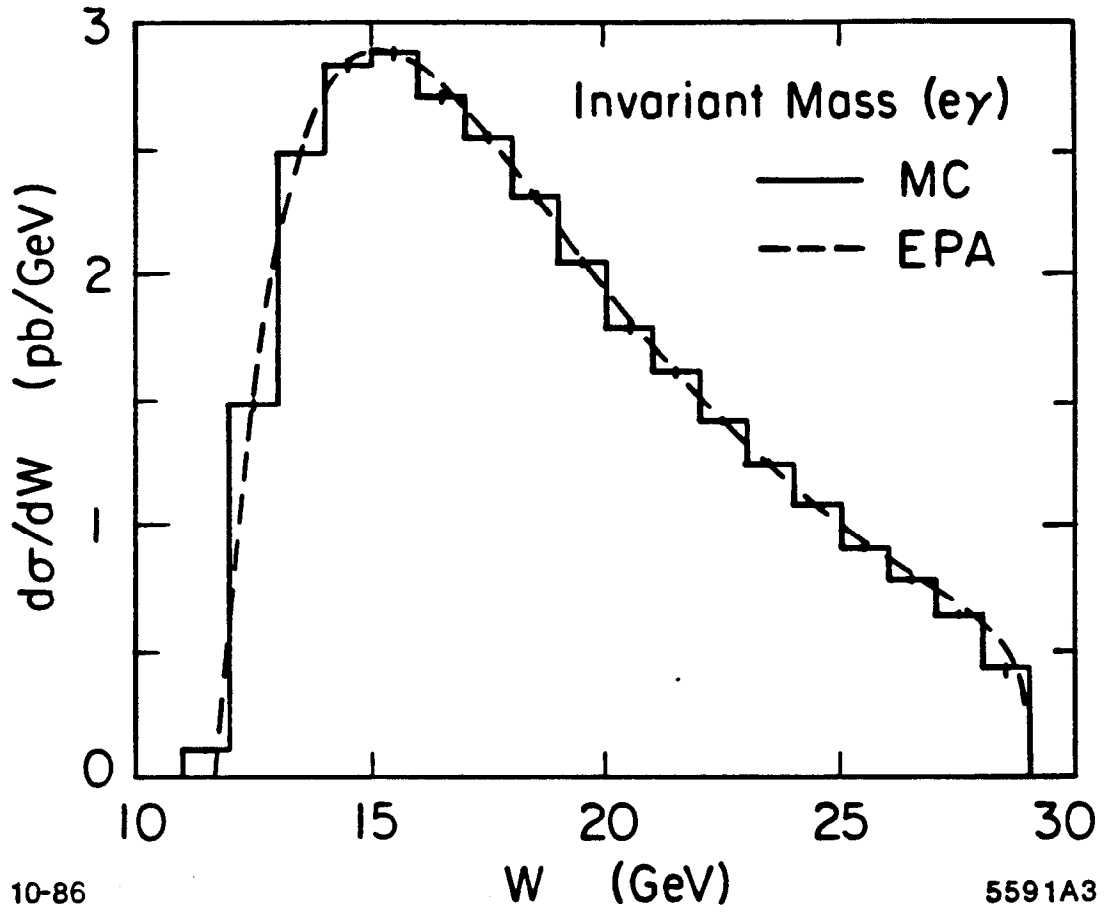

Figure 3. $e\gamma$ invariant mass distribution calculated to lowest order for a typical PEP or PETRA experiment. $E_b = 14.5$ GeV, $\cos\theta_{e\,\mathrm{min}} = \cos\theta_{\gamma\,\mathrm{min}} = 0.72$, $\theta_{e\,\mathrm{veto}} = 0.1$ rad. The dashed curve is from an EPA calculation, and the histogram is from the Monte Carlo generator. The total cross section is calculated from the EPA to be 29.51±0.01 pb and from the Monte Carlo to be 29.29±0.07 pb.

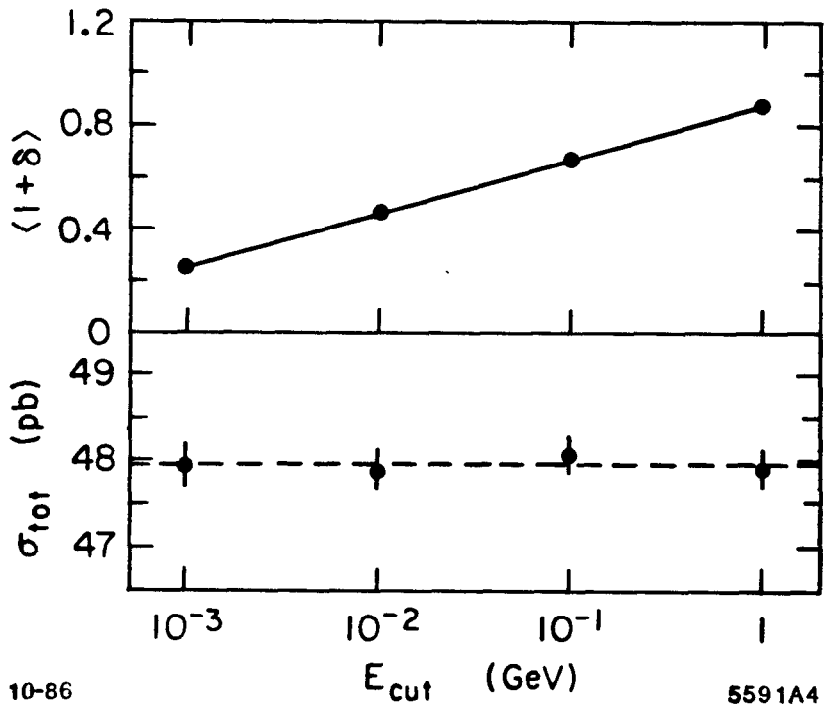

Figure 4. The average virtual and soft correction, $\langle 1 + \delta \rangle$, and the order α^4 total cross section for various cutoff energies for the experiment described in fig. 3 with $E_{\gamma\,\mathrm{min}} = E_{e\,\mathrm{min}} = 1$ GeV and the $e\gamma$ separated by more than 45° in ϕ.

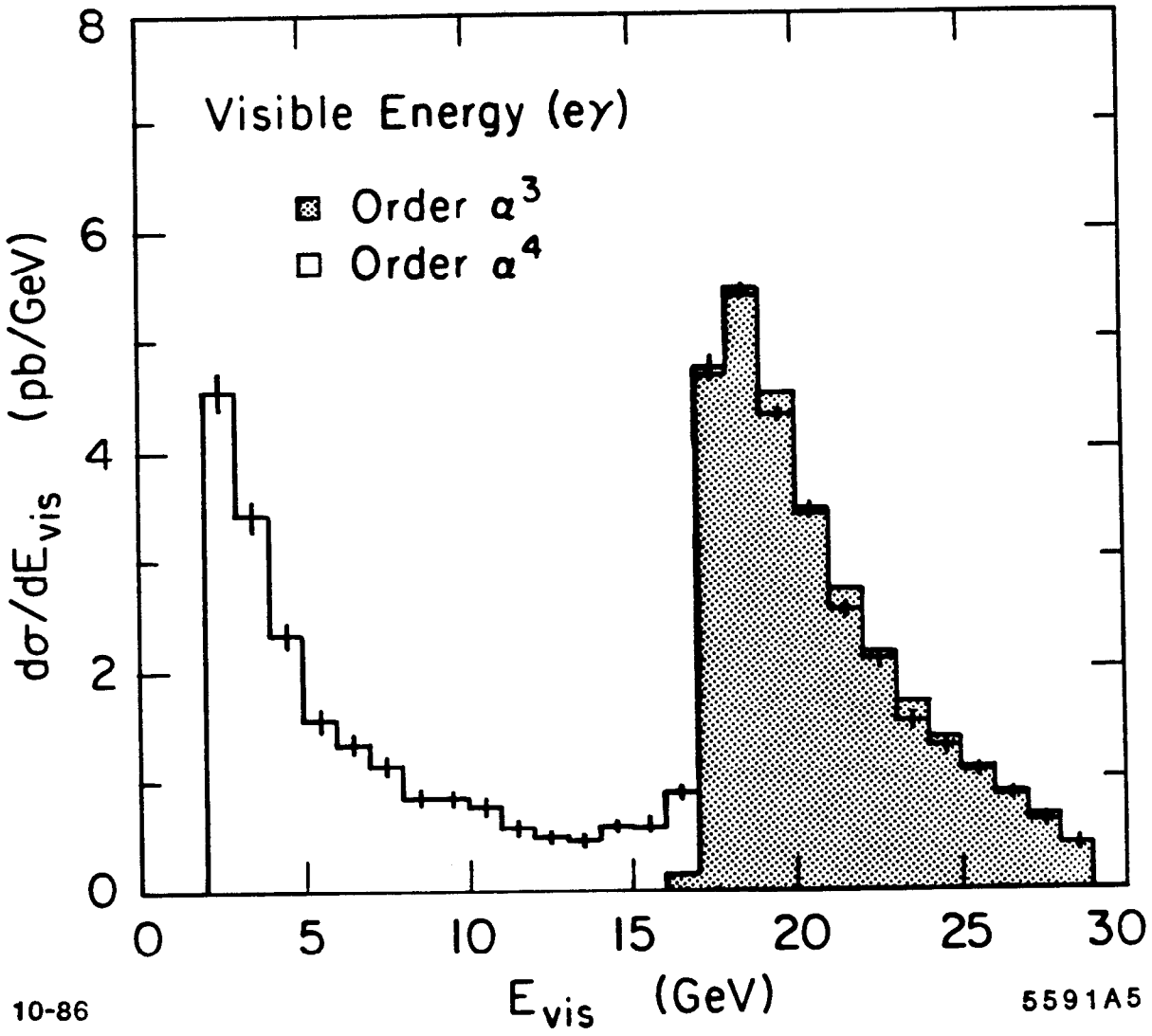

Figure 5. Total energy in the detector for the experiment described in fig. 4. The shaded histogram is the order α^3 result and the unshaded is order α^4. The order α^3 total cross section is calculated to be 29.29 ± 0.07 pb ; the order α^4 to be 47.95 ± 0.12 pb.

Table 1. Single photon cross sections for a simple SLC or LEP experiment. $E_b = 47$ GeV, $\theta_{\gamma\,\mathrm{min}} = 30°$, $\theta_{e\,\mathrm{veto}} = 15$ mrad. For the order α^4 cross section, $\theta_{\gamma\,\mathrm{veto}} = 15$ mrad. Only statistical errors are included.

$E_{\gamma\,\mathrm{min}}$	0.5 GeV	1.0 GeV	1.5 GeV
Description	σ_{tot} (pb)		
Order α^3 2 diagrams	33.40 ± 0.09	4.89 ± 0.03	0.120 ± 0.003
Order α^3 complete	34.24 ± 0.09	5.06 ± 0.02	0.145 ± 0.003
Order α^4	34.33 ± 0.10	4.77 ± 0.03	0.132 ± 0.003

diagrams, we have simulated the single γ process for a simple SLC or LEP experiment. The total cross section is given in table 1 calculated to the lowest order using the complete cross section, given by eq. (2.4), as well as using only the two diagrams shown in fig. 1, given by eq. (2.3). In the cases where one electron is allowed scatter at 0° ($E_{\gamma\,\mathrm{min}} = 0.5$ and 1.0 GeV), the two cross sections agree to about 3%, which again indicates the interference and annihilation terms are small and the method used for the next order correction is valid. When the criteria force both electrons to be away from 0° ($E_{\gamma\,\mathrm{min}} = 1.5$ GeV), the agreement is worse. In this case, the approximation used for the next order correction is less accurate. Table 1 also shows the total cross section when the order α^4 diagrams are included. The correction is seen to be very small.

In summary, we have presented a method to simulate radiative Bhabha scattering for configurations where one or both electrons scatter at small angles. We have shown that for the $e\gamma$ configuration, the effect of including order α^4 can be large, due to low visible energy topologies that are kinematically inaccessable by three body final states. The size of this correction is best understood by the fact that if an electron radiates a hard photon in the initial state, the γe scattering process can take place at a much reduced center of mass energy. By specifying a minimum total visible energy, the correction can be reduced. The order α^4 correction to the single photon configuration has been shown to be very small.

The author wishes to thank Manel Martinez and Ramon Miquel for very useful discussions which assisted in discovering an error in the event generation procedure. They have completed a calculation [21] of double radiative Bhabha scattering and find good agreement with the EPA method presented here.

APPENDIX

Some lengthy formulas referenced in the text are included here. The lowest order cross section for radiative Bhabha scattering from ref. [5] is given by

$$
\begin{aligned}
d^5\sigma_{\rm BK} &= \frac{\alpha^3}{\pi^2 s} A W_{\rm IR} W_{\rm m}\, d^5\Gamma \\
A &= (ss'(s^2+s'^2)+tt'(t^2+t'^2)+uu'(u^2+u'^2))/(ss'tt'), \\
W_{\rm IR} &= \frac{s}{x_1x_2}+\frac{s'}{y_1y_2}-\frac{t}{x_1y_1}-\frac{t'}{x_2y_2}+\frac{u}{x_1y_2}+\frac{u'}{x_2y_1}, \\
W_{\rm m} &= 1-\frac{m_e^2(s-s')}{s^2+s'^2}\left(\frac{s'}{x_1}+\frac{s'}{x_2}+\frac{s}{y_1}+\frac{s}{y_2}\right).
\end{aligned}
\tag{A1}
$$

The correction term for virtual and real soft photon emission for Compton scattering from ref. [15] with four misprints removed is

$$
\begin{aligned}
\delta^{\rm cm}_{\gamma e^-\to\gamma e^-} = -\frac{\alpha}{\pi U}\Bigg\{ & 2(1-2y)U\ln(2\frac{E_{\rm cut}}{m_e})+\frac{\pi^2}{6}\left(4-3t-\frac{1}{t}-\frac{2}{E^4t^3}\right) \\
& +4(2-U)y^2-4y+\tfrac{s}{2}U+\frac{2}{E^2t^2}+4\left(1-\frac{1}{2t}\right)\ln^2 E \\
& +\left(2t+\frac{1}{t}-2+\frac{2}{E^4t^3}\right)L_2(1-E^2t) \\
& +\left[2-5t-\frac{2}{t}+4y\left(\frac{2}{t}+t-2\right)\right]\ln E \\
& -\tfrac{1}{2}U\ln^2(1-t)-UL_2(t) \\
& +\left[1-\frac{2}{t}-\frac{2}{E^2t^2}-\frac{\frac{1}{2}E^2}{1-E^2t}+4y\left(t-1+\frac{1}{2t}\right)\right]\ln(E^2t)\Bigg\},
\end{aligned}
\tag{A2}
$$

$$
E=\frac{\sqrt{\tilde{s}}}{m_e}, \quad t=\tfrac{1}{2}(1+\beta_-\cos\theta_k^{\rm cm}), \quad y=\ln\left[E\sin(\tfrac{1}{2}\theta_k^{\rm cm})\right], \quad U=t+1/t,
$$

where $L_2(x)$ is the second order Spence function,

$$
L_2(x) = -\int_0^1 \frac{\ln u}{\frac{1}{x}-u}\,du. \tag{A3}
$$

The matrix element for double Compton scattering calculated in ref. [16], appears in ref. [20] as

$$
\begin{aligned}
X_{\rm MS} &= 2(ab-c)\left[(a+b)(x+2)-(ab-c)-8\right]-2x(a^2+b^2)-8c \\
&+\frac{4x}{AB}\left[(A+B)(x+1)-(aA+bB)(2+z\frac{1-x}{x})+x^2(1-z)+2z\right] \\
&-2\rho[ab+c(1-x)]
\end{aligned}
$$

$$
a=\sum_1^3\frac{1}{\kappa_i},\quad b=\sum_1^3\frac{1}{\kappa_i'},\quad c=\sum_1^3\frac{1}{\kappa_i\kappa_i'},
$$

$$
x=\sum_1^3\kappa_i,\quad y=\sum_1^3\kappa_i',\quad z=\sum_1^3\kappa_i\kappa_i', \tag{A4}
$$

$$
A=\kappa_1\kappa_2\kappa_3,\quad B=\kappa_1'\kappa_2'\kappa_3'\quad \rho=\sum_1^3\left(\frac{\kappa_i}{\kappa_i'}+\frac{\kappa_i'}{\kappa_i}\right),
$$

$$
m_e^2\kappa_1=p_-\cdot k,\quad m_e^2\kappa_2=p_-\cdot k_s,\quad m_e^2\kappa_3=-p_-\cdot\tilde{k},
$$

$$
m_e^2\kappa_1'=-q_-\cdot k,\quad m_e^2\kappa_2'=-q_-\cdot k_s,\quad m_e^2\kappa_3'=q_-\cdot\tilde{k}.
$$

REFERENCES

[1] E. Ma and J. Okada, Phys. Rev. Lett. 41 (1978) 287;
K. Gaemers, R. Gastmans and F. Renard, Phys. Rev. D19 (1979) 1605;
G. Barbiellini, B. Richter and J. L. Siegrist, Phys. Lett. 106B (1981) 414

[2] M. K. Gaillard, I. Hinchliffe and L. Hall, Phys. Lett. 116B (1982) 279;
P. Fayet, Phys. Lett. 117B (1982) 460;
J. Ellis and J. Hagelin, Phys. Lett. 122B (1983) 303

[3] H. Terazawa, M. Yasuè, K. Akama and M. Hayashi, Phys. Lett. 112B (1982) 387;
K. Hagiwara and D. Zeppenfeld, Z. Phys. C29 (1985) 115

[4] A. Courau and P. Kessler, Phys. Rev. D33 (1986) 2024

[5] F. A. Berends and R. Kleiss, Nucl. Phys. B228 (1983) 537

[6] F. A. Berends, R. Kleiss, P. De Causmaecker, R. Gastmans and T. T. Wu, Phys. Lett. 103B (1981) 124

[7] A. C. Hearn, REDUCE, version 3.2 (The Rand Corporation, 1985)

[8] S. M. Swanson, Phys. Rev. 154 (1967) 1601

[9] F. A. Berends, P. De Causmaecker, R. Gastmans, R. Kleiss, W. Troost and T. T. Wu, Nucl. Phys. B264 (1986) 265

[10] G. Bonneau and F. Martin, Nuovo Cim. 21A (1974) 611;
V. Gorgé, M. Locher and H. Rollnik, Nuovo Cim. 27 (1963) 928

[11] Y. S. Tsai, Phys. Rev. 120 (1960) 269

[12] W. L. van Neerven and J. A. M. Vermaseren, Phys. Lett. 142B (1984) 80

[13] F. Bloch and A. Nordsieck, Phys. Rev. 52 (1937) 54

[14] F. A. Berends, P. H. Daverveldt and R. Kleiss, Nucl. Phys. B253 (1985) 421

[15] K. J. Mork, Phys. Rev. A4 (1971) 917; and private communication

[16] F. Mandle and T. H. R. Skyrme, Proc. Roy. Soc. A215 (1952) 497

[17] L. M. Brown and R. P. Feynman, Phys. Rev. 85 (1952) 231

[18] M. Caffo, R. Gatto and E. Remiddi, Phys. Lett. B173 (1986) 91;
Nucl. Phys. B286 (1987) 293

[19] C. Mana and M. Martinez, Nucl. Phys. B, to be published;
F. A. Berends, private communication

[20] J. M. Jauch and F. Rohrlich, The theory of photons and electrons
(Springer, New York, 1955) p. 237

[21] M. Martinez and R. Miquel, UAB-LFAE preprint 87-01 (1987); and private
communication